On the Occurrence of GPS Signal Amplitude Degradation for Receivers on Board LEO Satellites

Xiong, Chao; Xu, Ji Sheng; Stolle, Claudia; van den Ijssel, Jose; Yin, Fan; Kervalishvili, Guram N.; Zangerl, Franz

DOI
10.1029/2019SW002398

Publication date
2020

Document Version
Final published version

Published in
Space Weather

Space Weather

RESEARCH ARTICLE
10.1029/2019SW002398

On the Occurrence of GPS Signal Amplitude Degradation for Receivers on Board LEO Satellites

Chao Xiong[1], Ji-Sheng Xu[2], Claudia Stolle[1], Jose van den Ijssel[3], Fan Yin[2], Guram N. Kervalishvili[1], and Franz Zangerl[4]

[1]GFZ German Research Centre for Geosciences, Potsdam, Germany, [2]Department of Space Physics, College of Electronic Information, Wuhan University, Wuhan, China, [3]Faculty of Aerospace Engineering, Delft University of Technology, Delft, Netherlands, [4]RUAG Space GmbH, Vienna, Austria

Key Points:
- Strong phase variation but no amplitude degradation is observed for GPS receivers on board CHAMP and Swarm satellites during scintillation
- Strong phase variation and amplitude degradation (of about 15 dB Hz) are both observed for the GPS receiver on board GOCE flying at a lower altitude
- The result suggests that the Fresnel diffractive process is necessary to cause GPS signal amplitude fades during scintillation

Correspondence to:
C. Xiong,
bear@gfz-potsdam.de

Citation:
Xiong, C., Xu, J.-S., Stolle, C., van den Ijssel, J., Yin, F., Kervalishvili, G. N., & Zangerl, F. (2020). On the occurrence of GPS signal amplitude degradation for receivers on board LEO satellites. *Space Weather*, *18*, e2019SW002398. https://doi.org/10.1029/2019SW002398

Received 7 NOV 2019
Accepted 19 JAN 2020
Accepted article online 22 JAN 2020

Abstract Transient signal loss of the global positioning system (GPS) has been frequently observed by receivers on board the European Space Agency's Swarm mission when the satellites encounter ionospheric plasma irregularities. In this study we provided the first comparison of the GPS signal amplitude degradations from receivers on board low Earth orbiting satellites at different altitudes. Intense carrier phase variations but almost no amplitude fades (less than 2 dB Hz) are observed when the spaceborne receiver lies right inside the ionospheric plasma irregularities, like the case for the Swarm and CHAMP satellites flying at about 400–500 km. This indicates that the strong phase variation, but not the amplitude fades, causes the receivers to stop tracking the GPS signals. When the receiver is located 100–200 km below the slab of plasma irregularities, like the case for the GOCE satellite flying at about 250 km, signal amplitude fades exceeding 10 dB Hz are observed, in addition to strong phase variation. Our results suggest that a considerable distance of the receiver to the plasma irregularity slab is needed to affect the Fresnel diffractive process and further causes GPS signal amplitude fades.

1. Introduction

Plasma irregularities are an important subject for ionospheric studies, as they can cause disturbances of the transionospheric radio wave signals. When propagating through Earth's ionosphere, the radio waves interact with free electrons along the transmission paths, introducing group delay and phase advance (Kintner et al., 2007). When the radio waves strike a volume of plasma irregularities, rapid fluctuations of the carrier phase and amplitude are usually observed from ground-based receivers, which is also called ionospheric scintillations. With the development of global navigation satellite systems (GNSS) in the past decades, scintillation on the L-band frequency has been widely investigated (e.g., Aarons, 1982; Aarons & Basu, 1994; Basu et al., 1980; Bhattacharyya et al., 2014; Kintner et al., 2007). From a global view, ionospheric scintillations are most frequently observed at the equatorial and low latitudes, as well as at the polar region. Severe scintillations can degrade the tracking performance of a receiver in terms of cycle slips and increased navigation error or even cause the receiver to stop tracking. Such transient stop tracking of GNSS signal is due to the carrier phase variation being out of range of a technically set phase-locked loop (PLL), or the received signal amplitude being lower than a preset threshold, or the phase/amplitude variations being too fast to be tracked.

The GNSS signals are only affected by scintillations when plasma irregularities are present in their propagating paths. As plasma irregularities, with horizontal extension from meters to hundreds of kilometers, exist mainly at a few hundred kilometers above the Earth's surface, in most cases of scintillation only some of the tracked GNSS signals will be affected for the receivers at ground. However, for receivers on board low Earth orbiting (LEO) satellites, the tracked GNSS signals from all directions are often affected when the LEO satellites fly inside the plasma irregularities. Transient signal loss/interruption at all channels from the global positioning system (GPS) receivers on board European Space Agency's Gravity field and Steady-state Ocean Circulation Explorer (GOCE) mission as well as the Swarm mission have been reported (van den Ijssel et al., 2011; Xiong, Stolle, & Lühr, 2016).

Scintillation observed by ground-based receivers exhibits usually as rapid fluctuations on both carrier phase and signal amplitude that are represented by the scintillation indices, σ_ϕ and S_4, respectively (e.g., Pi et al.,

1997; Van Dierendonck et al., 1993). One cannot fully separate the influences of phase and amplitude variations on the tracking performance of ground-based receivers, as the deepest amplitude fades usually occur during the fastest phase variations. However, Sust et al. (2014) found that the GPS receiver on board Swarm showed strong phase scintillation but no discernable fluctuations on the signal amplitude (carrier-to-noise-density ratio, C/N_0) when loss-of-lock incidents happened. This is also evidenced in Figure 1 of Xiong, Stolle, and Lühr (2016); when transient GPS signal losses were observed at all tracking channels of Swarm, almost no fades of C/N_0 were observed. A recent work from Xu et al. (2018) provided simulations of the phase and amplitude scintillations for GPS receivers on board a LEO satellite, by using a two-component power law phase screen model (e.g., Carrano & Rino, 2016). They showed that when a LEO satellite is inside the plasma irregularities, only phase scintillation but no amplitude scintillation can be observed. However, when the phase screen in the model is moved further above the LEO satellite, the amplitude scintillation, S_4, starts to increase gradually and reaches a saturation value of 0.8 when the phase screen is located at 100–200 km above the LEO satellite.

Until now, the model simulation of Xu et al. (2018) has not been verified by using real GNSS measurements that are located at different distances with respect to the irregularity slab. GNSS receivers on board LEO missions that orbit the Earth at different altitudes provide a good opportunity for such a purpose. In this study, we provide the first comparison of GPS signal amplitude variations from receivers on board LEO satellites at different altitudes: the Swarm satellites at about 450 km, the Challenging Minisatellite Payload (CHAMP) at about 400 km, and the GOCE satellite at about 250 km. In addition, the GPS measurements from a ground-based receiver located in southern China have also been used for comparison. In the section to follow, we first introduce the three LEO missions and their onboard GPS receivers. An example and statistical results of the amplitude variations when the satellites encounter plasma irregularities are given in section 3. Relevant discussions taking into account previous studies are given in section 4. Section 5 provides our main findings.

2. Data Set

The Swarm mission, comprising three spacecraft, was launched on 22 November 2013 into a near-polar (87.5° inclination) orbit with initial altitude of about 500 km. From January 2014 onward, the three spacecraft were maneuvered apart and achieved their final constellation on 17 April 2014. From then on, the lower pair (Swarm A and C) is flying side by side with a longitudinal separation of about 1.4°, at an altitude of about 470 km. The third spacecraft, Swarm B, orbits the Earth at about 520 km with a higher inclination of 88°. All three Swarm satellites carry dual-frequency GPS receivers of the same type developed by RUAG Space (Zangerl et al., 2014). The GPS receivers are equipped with eight channels for dual-frequency tracking, which means that the Swarm satellites can simultaneously receive signals from at most eight GPS satellites. During the earlier mission period, all three Swarm satellites delivered GPS data with a time resolution of 10 s, but on 15 July 2014 the receiver configuration was changed, and since then all Swarm satellites are delivering 1 Hz GPS measurements. More detailed information about the technical updates of the Swarm receivers was described by van den Ijssel et al. (2016).

The CHAMP satellite was launched on 15 July 2000, into a near-circular polar orbit (87.3° inclination) with an initial altitude of 456 km. The satellite reentered Earth's atmosphere on 19 September 2010. The primary objectives of CHAMP comprise the accurate determination of the Earth's magnetic and gravitational fields, as well as collecting measurements from the ionosphere and upper atmosphere (Reigber et al., 2002). Among a number of highly accurate instruments, a BlackJack GPS receiver designed by the Jet Propulsion Laboratory was equipped for precise orbit determination (POD) of CHAMP. The GPS measurements were delivered with a time resolution of 10 s. At the beginning of the mission, only eight channels were activated for POD, but after a software update on 5 March 2002, the tracking channels for POD have been increased to 10. Detailed information about the CHAMP GPS receiver can be found in Montenbruck and Kroes (2003).

The GOCE satellite was launched on 17 March 2009, into a near-circular dusk-dawn Sun-synchronous orbit (96.7° inclination) with an initial altitude of 283 km. The satellite reentered Earth's atmosphere on 11 November 2013. The core instrument of GOCE was a three-axis gradiometer for determining the Earth's gravitational field (Rummel et al., 2002). In addition, GOCE was equipped with two 12-channel dual frequency Laben Lagrange GPS receivers for POD (Montenbruck et al., 2006). The main receiver was

running in nominal operations and delivered 1 Hz GPS measurements, whereas the other one served as a redundant unit (Bock et al., 2011). The extremely low altitude, down to 224 km at the end of the mission, makes GOCE unique compared to other LEO missions.

In addition to observations from the above mentioned LEO satellites, GPS measurements from one station located in southern China, at Nanning (geographic latitude and longitude: 22.84°N and 108.23°E, magnetic latitude: 13.08°N) have also been used for comparison. The station is equipped with a NovAtel GSV4004B receiver, which offers 24 channels for tracking dual-frequency GNSS signal and delivers 20 Hz measurements. More detailed information of this station is given in Cheng et al. (2018).

3. Observations

3.1. Features of GPS Signal Amplitude Degradation From Receivers at Ground Level

Figure 1a presents the trajectories of visible GPS satellites from the Nanning station (marked with a black pentagon), during 11:30–13:30 Coordinated Universal Time (UTC) on 14 March 2015, when prominent ionospheric scintillations were observed. The height of the ionospheric piercing points of the visible GPS satellites with respect to the station is set to 400 km. The pseudorandom noise (PRN) code of each visible GPS satellite is labeled, and the direction of its trajectory is marked with a blue arrow. The color of the trajectory represents the intensity of amplitude scintillation index, S_4, measured by the ground-based receiver. The S_4 index is calculated at each 1-min interval. Amplitude scintillation with $S_4 > 0.3$ mainly occurs for the GPS satellites located southward of the station, for example, PRN = 01, 04, 09, 23, but is also visible for PRN = 16 and 19 at geographic latitude higher than 25°. The most severe scintillation (with $S_4 > 0.6$) during this period is observed for PRN = 16, at regions close to the East China Sea. However, there are also signals from GPS satellites, like PRN = 17, 11, 27, 28, and 30, showing almost no amplitude scintillation.

Figure 1b presents the carrier phase and signal amplitude on the L1 frequency (1,575.42 MHz) of GPS satellite PRN = 04 during the considered 2-hr interval. From top to bottom this figure shows the elevation angle, the detrended and high-pass-filtered (cutoff frequency at 0.1 Hz) carrier phase ($\Delta\phi$), the detrended signal amplitude ($\Delta C/N_0$), the slant total electron content (STEC), and the phase and amplitude scintillation index, σ_ϕ and S_4, respectively. Similar to S_4, σ_ϕ is calculated at each 1-min interval. Both the σ_ϕ and S_4 show prominent fluctuations between 12:00 and 12:50 UTC and reach as high as 1.5 and 0.5, respectively. The STEC decreases and shows also fluctuations during this interval. Figure 1c presents more detailed variations of $\Delta\phi$ and $\Delta C/N_0$ of PRN = 04 during a 1-min interval (12:37:30-12:38:30 UTC). We see clearly that larger degradation of C/N_0 occurs when larger $\Delta\phi$ is observed. Around 12:37:38 UTC, the degradation of C/N_0 reaches as much as 20 dB Hz. Under such strong scintillation, the signal from PNR = 04 was interrupted five times (indicated by the red arrows) within the 1-min interval.

3.2. Examples of GPS Signal Amplitude Degradation Derived From Receivers on Board LEO Satellites at Different Altitudes

Around 12:43 UTC on the same day, Swarm A and C flew over the Nanning station at about 450 km (see their trajectories in Figure 1a, represented by the magenta and black dash-dot lines, respectively). Figure 2a presents the in situ electron density measured by the onboard Langmuir probe, and the number of tracked GPS satellites from Swarm A. The electron density shows a well-formed equatorial ionization anomaly (EIA), with two crests around ±18° magnetic latitude (MLAT) and a trough above the dip equator. Compared to the small-scale depletions at the EIA northern crest, the depletions at the southern crest are much stronger. As a result, the tracked GPS satellites are reduced from eight to three at the southern crest region. For the POD of Swarm, the number of tracked GPS satellites should not be less than four; therefore, the epochs with tracked GPS satellites less than four are marked with red color. Figure 2b shows the simultaneous observations from Swarm C, which flies 1.4° eastward of Swarm A. Although the background electron density measured by the two satellites is similar, they probe small-scale plasma irregularities of different structures. Overall, Swarm C observes much stronger depletions at the crests and above the dip equator. Such differences observed by the closely flying Swarm satellites are due to the fact that the postsunset equatorial plasma irregularities usually have longitudinal extensions less than 50 km, which has been discussed in detail by Xiong, Stolle, Lühr, Park, et al. (2016), Xiong, Xu, et al. (2018).

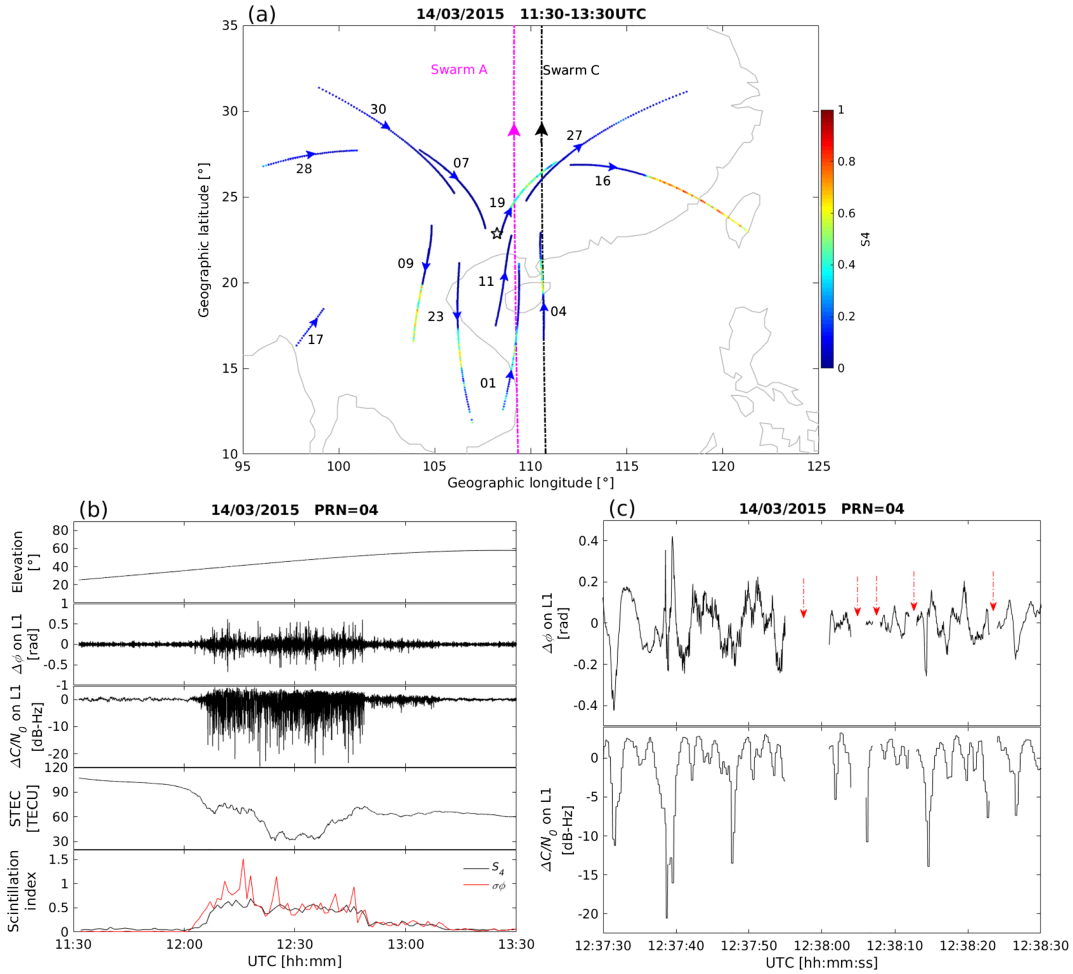

Figure 1. (a) The trajectories of visible GPS satellites from one ground-based station (marked with a black pentagon) located at Nanning, China, on 14 March 2015. The color of the trajectory represents the intensity of the amplitude scintillation index, S_4. (b) The variation of elevation angle, the detrended and high-pass-filtered carrier phase ($\Delta\phi$) and detrended signal amplitude ($\Delta C/N_0$) on the L1 frequency, the STEC, and the phase and amplitude scintillation index, σ_ϕ and S_4, for the GPS satellite PRN = 04. (c) The variations of $\Delta\phi$ and $\Delta C/N_0$ from PRN = 04 in a 1-min interval.

For Swarm C, Figures 2c and 2d show the detrended and high-pass-filtered (cutoff frequency at 0.1 Hz) carrier phase ($\Delta\phi$) and C/N_0 on the L1 frequency (black), as well as the elevation angle (red) of each visible GPS satellite, respectively. We have applied high-pass filters with different cutoff frequencies to the carrier phase measurements, but as we focused only on their fluctuations, we finally selected the value, 0.1 Hz, that has been conventionally used for the ground-based receivers (e.g., Van Dierendonck et al., 1993). The epochs with dot-dashed lines indicate that the GPS signal is transiently interrupted. Fluctuations of $\Delta\phi$ are seen from almost all visible PRN at the EIA crest and trough regions, where the plasma depletions are observed. These fluctuations appear for both low- and high-elevation angles. However, no clear fluctuation of C/N_0 is observed for any PRN, which is different from the ground-based receiver (Figure 1b). Figure 2e shows the detailed variations of $\Delta\phi$ and C/N_0 for PRN = 03. Strong fluctuations of $\Delta\phi$ are found after 12:34 UTC. Here we would like to note that slight C/N_0 degradations with amplitude less than 1 dB Hz are observed when the elevation angle of PRN = 03 is less than 30°, possibly related to the multipath influence under low elevation angle. Similar fluctuations of $\Delta\phi$ are found for PRN = 04 (Figure 2f), most prominently at the EIA crest regions when the elevation angle is still larger than 45°. The C/N_0 also degrades by about 2 dB Hz (indicated by a red arrow) before the signal interruption occurred at 12:35 UTC. However, the simultaneous C/N_0 degradation of PRN = 04 from the ground-based receiver at Nanning station reaches as high as 15 dB Hz (not shown here). The comparison between Figures 1b and 2f indicates that when the signal from

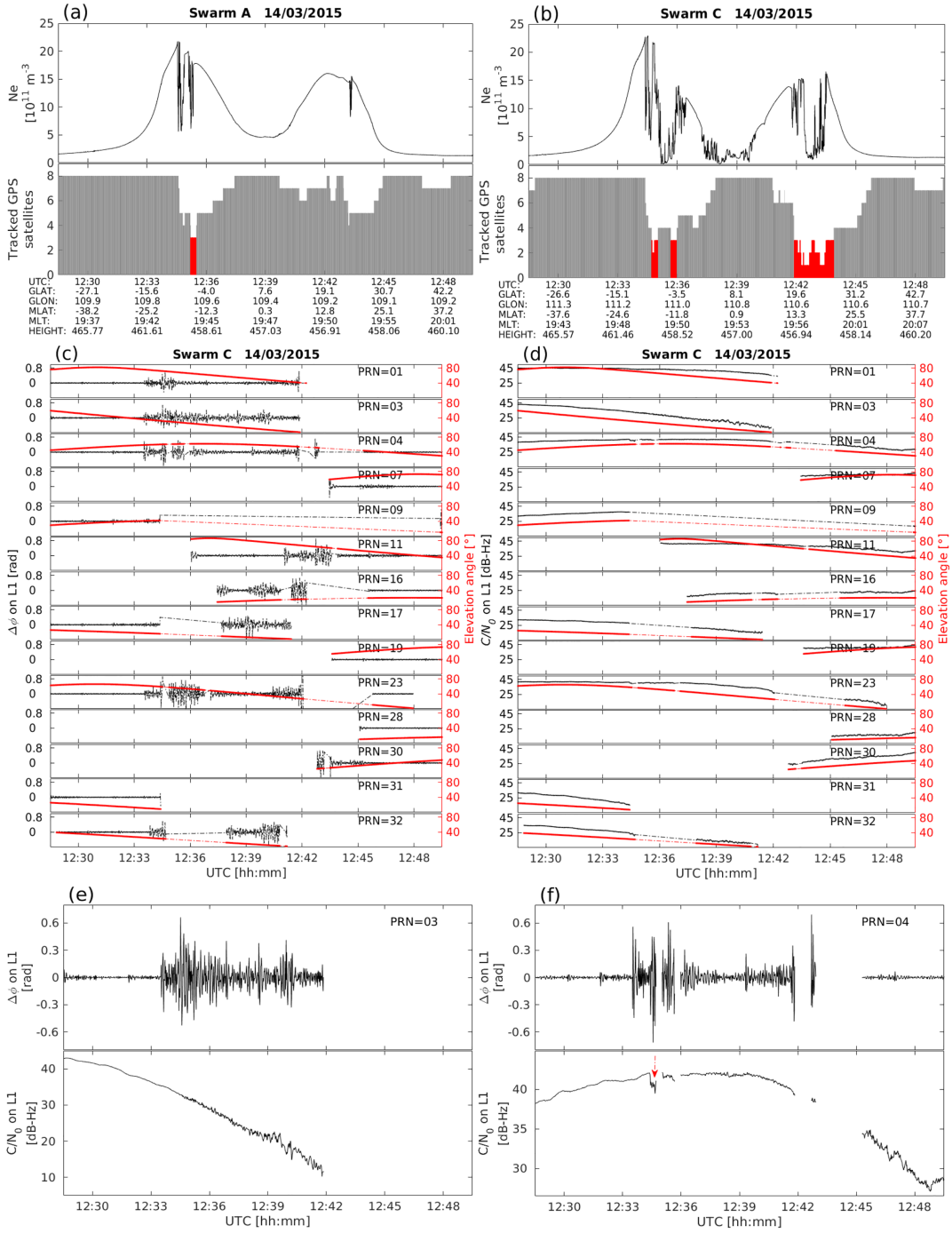

Figure 2. The in situ electron density and number of tracked GPS satellites from (a) Swarm A and (b) Swarm C on 14 March 2015. (c and d) The variations of $\Delta\phi$ and C/N_0 of visible GPS satellites observed by Swarm C, respectively. (e) and (f) are the $\Delta\phi$ and C/N_0 variations of PRN = 03 and 04, respectively.

the same GPS satellite (e.g., PRN = 04) is affected by the plasma irregularities, strong phase variations are seen from both ground-based and spaceborne receivers; however, only the ground-based receiver exhibits significant amplitude fades.

Figure 3 provides a similar example from the CHAMP satellite on 7 February 2002 when it flies at about 400 km. The top two panels show the in situ electron density measured by the onboard Langmuir probe and the number of tracked GPS satellites. The lower three panels show the elevation angle, the detrended

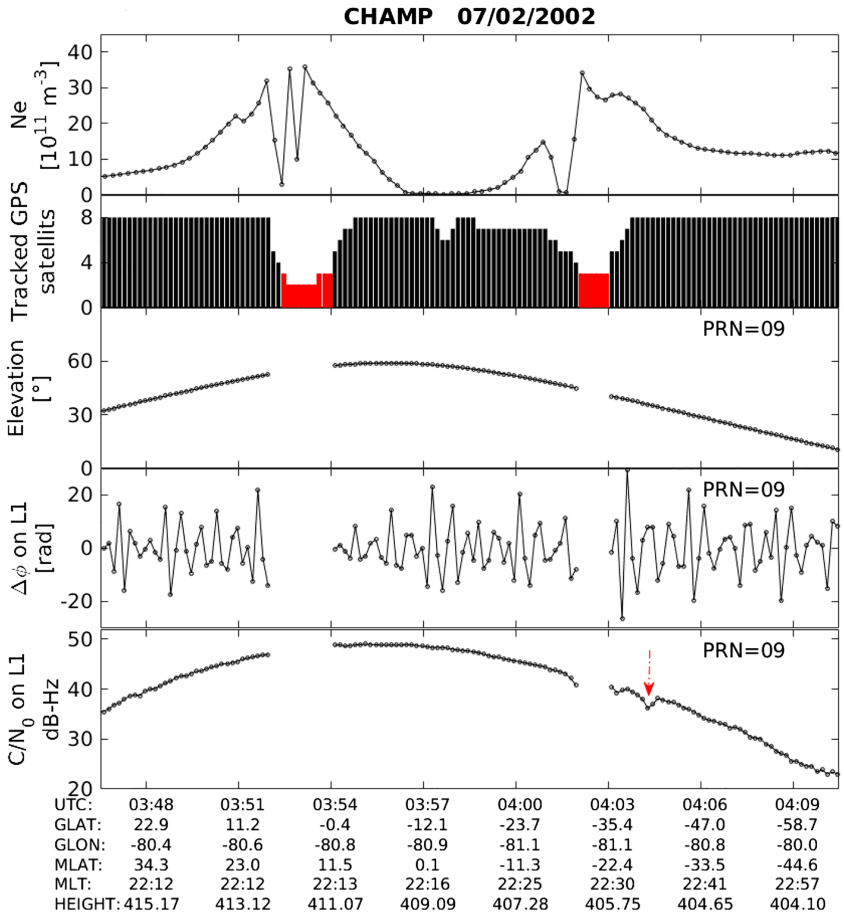

Figure 3. The in situ electron density and GPS measurements from the CHAMP satellite on 7 February 2002. The first and second panels show the in situ electron density and the tracked GPS satellite number, and the third to fifth panels show the elevation angle, $\Delta\phi$, and C/N_0 on the L1 frequency for GPS satellite PRN = 09.

and high-pass-filtered $\Delta\phi$, and the C/N_0 on the L1 frequency for tracked GPS satellite PRN = 09. When CHAMP encounters irregularities at both EIA crests, the tracked GPS satellite number reduces to less than four. We have to note that due to the lower time resolution of CHAMP GPS measurements (0.1 Hz), the cutoff frequency of the high-pass filter was set to 0.025 Hz. As a result, the derived $\Delta\phi$ varies within $\pm$20 rad, but fluctuations are still observable. Similar to the Swarm receiver, no clear amplitude degradation is observed from the C/N_0 of PRN = 09 before the GPS signal is interrupted. The most intense degradation of C/N_0 appears around 04:04 UTC, with an intensity of less than 2 dB Hz (indicated by a red arrow). The different types of GPS receivers on board the CHAMP and Swarm satellites share a common feature when they encounter strong irregularities in their orbit. The onboard GPS receivers show only strong carrier phase fluctuation but almost no amplitude fades. The result also suggests that the strong phase variation, but not the amplitude degradation, causes the GPS receivers on board LEO satellites, like Swarm and CHAMP, to stop tracking GPS satellites when they are located inside the plasma irregularities. This conclusion is consistent with the result of Xiong, Stolle, et al. (2018), who reported that the occurrence of GPS signal loss was reduced after the PLL bandwidth of the Swarm receivers was widened. For moderate scintillation when the carrier phase variation is still within the PLL bandwidth, the receiver can maintain tracking of GPS signals; however, when the phase variation is too large or too fast, the widened PLL bandwidth is helpless.

Figure 4a provides an example from the receiver on board GOCE satellite at about 255 km on 23 October 2012. From top to bottom the figure shows the STEC from GPS satellite PRN = 13, tracked GPS satellite number, the elevation angle, the detrended and high-pass-filtered carrier phase (cutoff frequency at 0.1 Hz), and

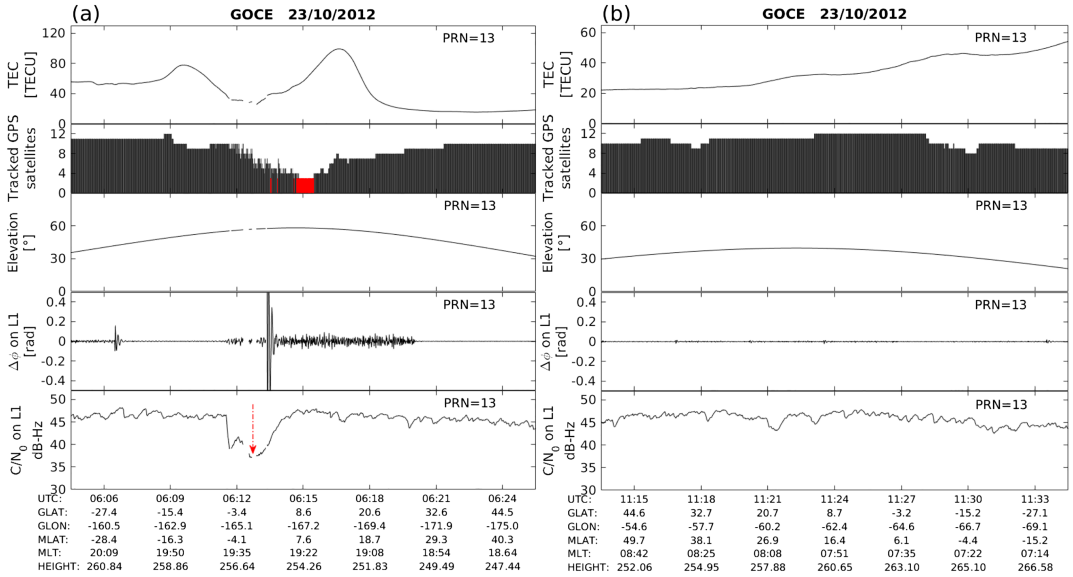

Figure 4. (a) Similar to Figure 3, but for one duskside orbit on 23 October 2012 from the GOCE satellite. As there is no in situ electron density measurements from GOCE, the STEC from GPS satellite PRN = 13 is shown in the first panel, and the fluctuations of STEC at the equatorial region indicates that the GPS ray from PRN = 13 propagates through the ionospheric irregularities. (b) Similar to (a), but for one dawnside orbit on the same day when no plasma irregularities are observed.

C/N_0 on the L1 frequency. The two crests of EIA are clearly visible from the STEC values on this duskside orbit, which shows also fluctuations close to the magnetic equator that should be related to the small-scale postsunset plasma irregularities, and the tracked GPS satellites reduce from 12 to 4. Strong fluctuations of $\Delta\phi$ are seen at equatorial latitudes, which is similar to the examples as observed by the Swarm and CHAMP satellites. Relatively slight fluctuation of $\Delta\phi$ is also observed around −28° MLAT, which is possibly caused by the plasma irregularities at middle latitude as the STEC shows also fluctuations at this latitude. Around 06:12 UTC degradation of signal amplitude by as much as 12 dB Hz is observed at latitudes close to the magnetic equator, which is similar to the behavior of the ground-based receiver. Slight fluctuations of C/N_0 are also observed at other latitudes, but they are within 2 dB Hz.

For comparison, Figure 4b provides another orbit of GOCE but on the dawnside. Similar results are shown from GPS satellite PRN = 13. The relatively smooth variation of STEC indicates that there are no plasma irregularities observed. As a result, neither phase fluctuation nor prominent signal amplitude degradation is observed, and the tracked GPS satellite number keeps more than eight during this period. It is worthy to notice that fluctuations of C/N_0 less than 2 dB Hz are also observed, which indicates that such slight fluctuations of the GPS signal amplitude from the GOCE onboard receiver should be not related to the ionospheric plasma irregularities.

3.3. Different Characteristics of GPS Signal Amplitude Degradation for Receivers on Board the Swarm and GOCE Satellites

To have a statistical comparison of the GPS signal amplitude degradation from LEO satellites at different latitudes, we focused on the Swarm C and GOCE satellites, as the GPS receivers from both missions deliver 1-Hz measurements. It is also known that the scintillations are more severe at higher solar flux level; therefore, we choose a 2-year period from August 2014 to July 2016 and from November 2011 to October 2013 for Swarm C and GOCE, respectively. We look at events when transient GPS signal interruptions (less than 10 min) occur. For each event, we use the midpoint between start and end of the interruption to represent its location. In addition, we take only the GPS measurements with elevation angle, α, larger than 45° into account, to reduce the influence of multipath.

The events from both satellites are first separately sorted into geographic latitude and longitude bins (5° × 15°), and within each bin the interruption events from all PRN are added up (Figures 5a and 5c). From a global view, GPS signal interruptions from Swarm C are mainly observed at low latitudes between

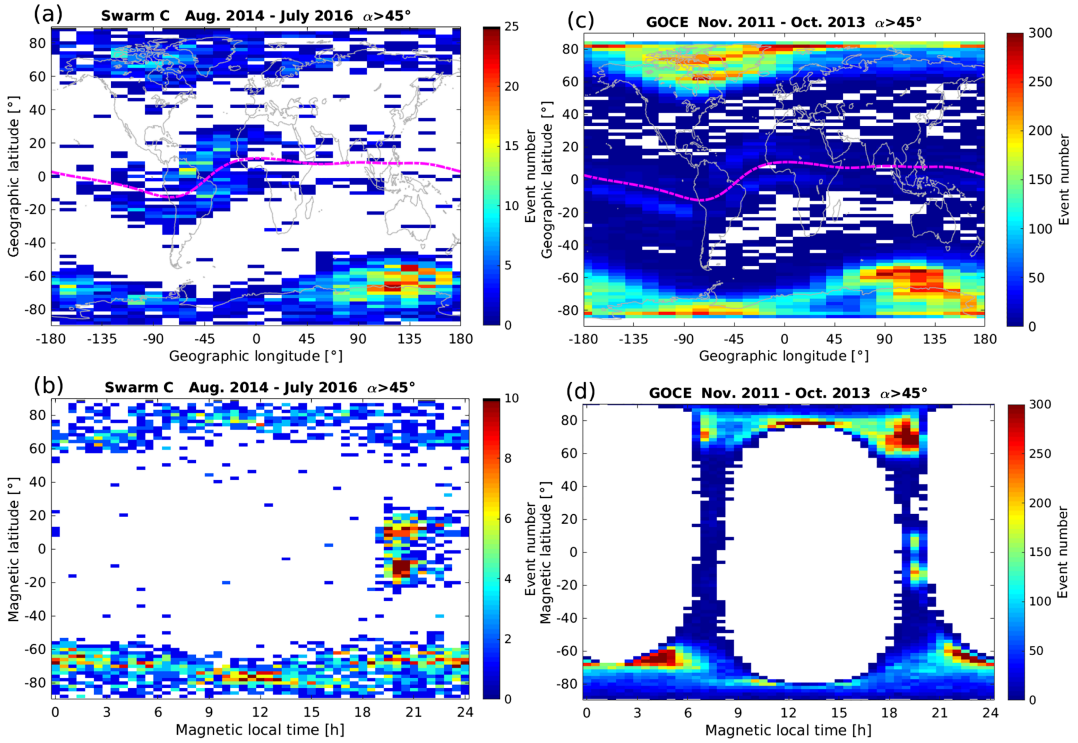

Figure 5. The (a) geographic latitude versus longitude distribution and (b) magnetic latitude versus magnetic local time distribution of the transient GPS signal interruption of Swarm C satellites, during a 2-year interval from August 2014 to July 2016. (c and d) The similar distributions but for the GOCE satellite from November 2011 to October 2013. For both satellites, only the GPS rays with elevation angle larger than 45° have been taken into account.

±5° and ± 20° MLAT (most prominent at longitudes between −135° and 0° E), as well as at the high latitude (most prominent at longitudes close to the magnetic poles). The GOCE result shows a similar global distribution, but the absolute number of GPS signal interruption is almost 10 times larger than that observed by Swarm C. We further look at their magnetic local time distribution, and the result is shown in Figures 5b and 5d. From both satellites, the low-latitude events appear mainly at postsunset hours and are nearly absent during the other local times, indicating the transient GPS signal interruption at low latitude is caused by the postsunset plasma irregularities. Although there are also low-latitude events observed at dawn hours from GOCE, they are much less (by a factor of 5) when compared to the events at the duskside. The high-latitude events generally have a wider local times distribution. The events around noon are located at higher latitudes and are collocated with the cusp region, while the nightside events prefer to appear at lower latitudes, and they should be collocated with the auroral oval. Similar magnetic local time distribution of transient GPS signal interruption from the Swarm satellites as well as their relation with high-latitude plasma irregularities have been investigated in detail by Xiong, Stolle, et al. (2018); therefore, we do not repeat the discussion here. GOCE satellite has only equatorial orbit crossings at dawn and duskside, but as the southern magnetic pole is located further away to the geographic pole when compared to the northern pole, GOCE can cover almost all the local time at southern high latitude. The nightside events at northern high latitude are confined to the dawn and dusk hours, while southern high-latitude events are somehow shifted toward later local times, and such difference should be caused by the orbit coverage of GOCE at high latitudes.

Figures 6a and 6d show the global distribution of the median value of C/N_0 from all PRN on the L1 frequency, for Swarm C and GOCE, respectively. Here, we only consider the periods when transient GPS signal interruption do not happen and used only measurements with elevation angle between the GPS satellite and Swarm/GOCE larger than 45°. The averaged C/N_0 shows almost constant value at all latitude and longitudes, with values of 41.6 and 46.0 dB Hz for Swarm C and GOCE, respectively, which can also be taken as background references for the two spaceborne receivers under situations of no ionospheric plasma

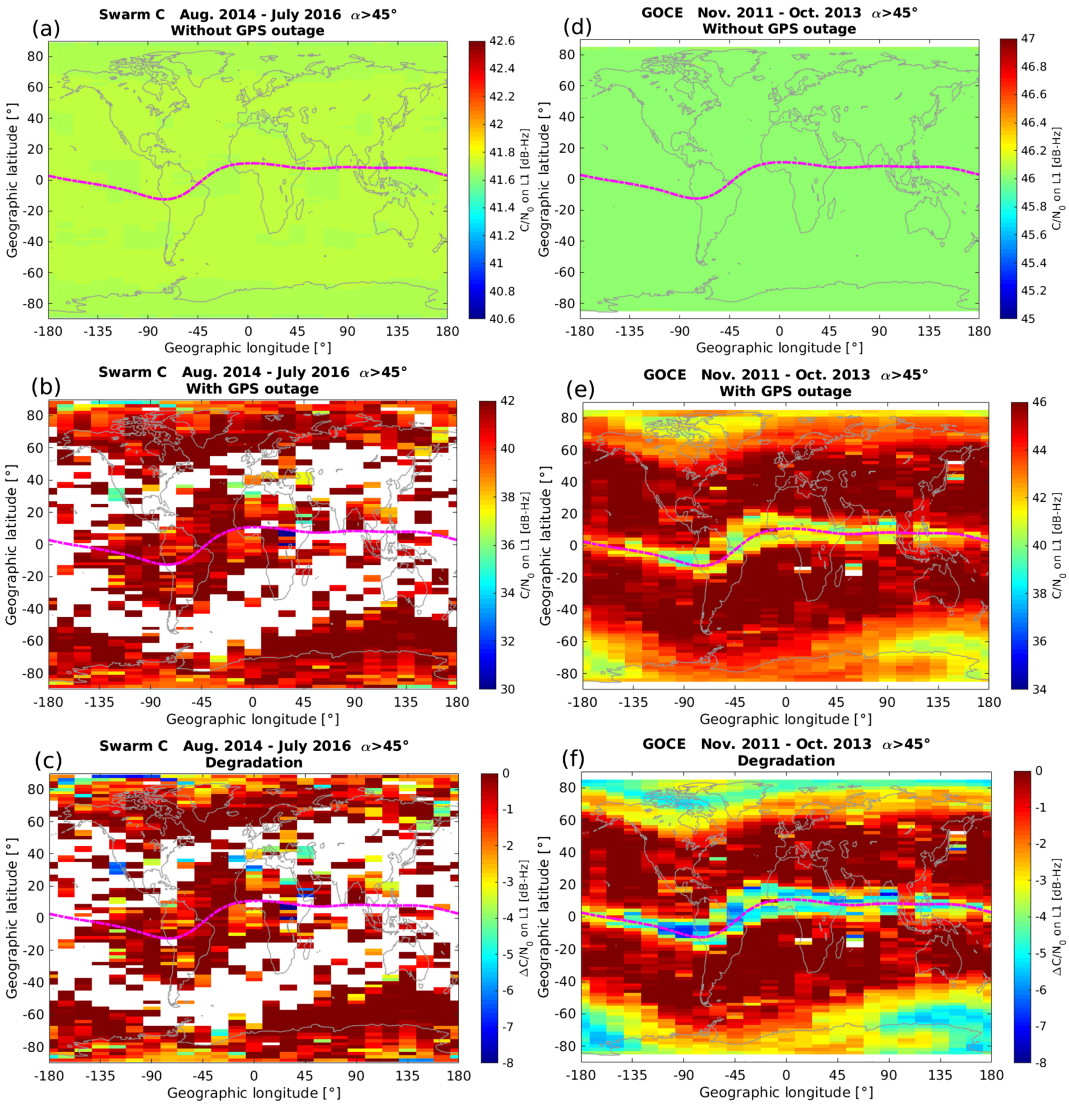

Figure 6. The global distributions of received GPS signal amplitude for Swarm C satellite under different situations: (a) without transient GPS signal interruption (b) only with transient GPS signal interruption. (c) The degradation of signal amplitude by subtracting (b) from (a). (d–f) Similar results but for the observations from GOCE satellite.

irregularities. For comparison, Figures 6b and 6e show the global distribution of the median value of C/N_0 when transient GPS signal interruptions happened. For each event, we considered only 30 s before/after the interruption start/end. From the Swarm C observation, no clear pattern of the C/N_0 can be found, but for the observations from GOCE, C/N_0 is found with lower value where more transient GPS signal interruptions happened. When subtracting the background reference, the degradation of signal amplitude, $\Delta C/N_0$, is shown in Figures 6c and 6f, and we see that on average $\Delta C/N_0$ reaches about 8 dB Hz at equatorial latitudes and regions close to the magnetic poles, but such feature cannot be seen from the observations of Swarm C. The statistical result is consistent with the examples as shown in our Figures 2 and 4. No prominent GPS signal amplitude degradation can be seen at the Swarm altitude, but an average degradation of about 8 dB Hz (or even larger for some cases) can be seen at the GOCE altitude.

One feature we want to point out is that there are also events from Swarm C, although very few, during which the $\Delta C/N_0$ can be occasionally lower than 30 dB Hz (see the randomly distributed bluish bins in Figures 6b and 6c). We further checked these events and show one example in Figure 7a. Swarm C encounters postsunset plasma irregularities at the low latitudes well reflected in electron density. The GPS signal interruptions at

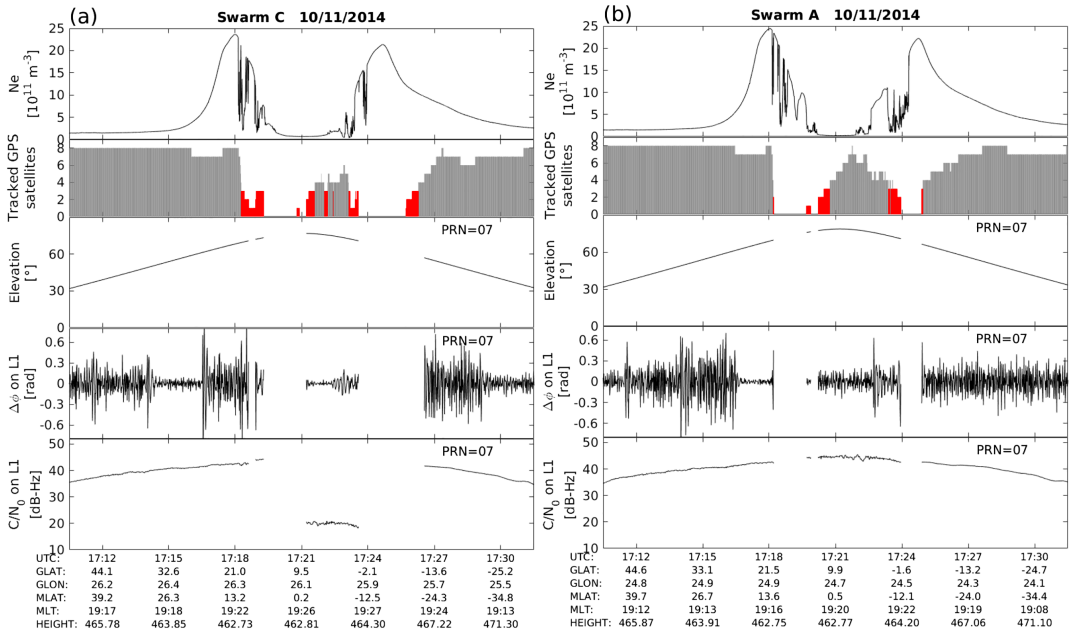

Figure 7. (a) An example of Swarm C satellite on 10 November 2014, during which the tracked GPS signal amplitude from PRN = 07 suddenly drops to below 20 dB Hz when transient GPS signal interruption happens, (b) but the GPS signal amplitude from the same PRN observed by the side-by-side flying Swarm A satellite does not show such a sudden drop.

all channels happen at the inner edge of EIA crests where plasma irregularities are strongest. Strong phase fluctuations and signal interruption are seen for PRN = 07, and from 17:21 to 17:24 UTC the signal amplitude drops as low as 20 dB Hz. However, this low signal amplitude suddenly drops to a very low level and then keeps almost constant, which is different from the situation as seen from GOCE onboard receiver that gradually decreases with time (Figure 4a). Furthermore, we check further observation from the side-by-side flying Swarm A, which encounters similar plasma irregularities and GPS signal interruptions. Strong carrier phase fluctuation from the same GPS satellite, PRN = 07, is also observed, but the signal amplitude keeps around 42 dB Hz and shows only fluctuation within 2 dB Hz. This comparison between Swarm A and C indicates that such occasional sudden drop of received signal amplitude to a very low value is possibly related to the hardware setting of Swarm C onboard receiver but not the scintillation effect.

4. Discussions

4.1. Radio Wave Propagation Through a Random Media and the Phase Screen Approximation

The study of ionospheric scintillation belongs to the problem dealing with the wave propagation through a random medium. Therefore, the scintillation problem can be solved by finding descriptions that map a point in the probability space of fluctuating media onto a point in the probability space of wavefield (e.g., Yeh & Liu, 1982). The starting point for developing the equations that describe radio wave propagation through a random scattering medium are the Maxwell's equations (e.g., Kintner et al., 2007). The result is typically the derivation of the scalar Helmholtz equation, which represents wave propagation in an irregular medium where single, forward scattering is predominant and where the irregularities have scale sizes larger than the wavelength of the radio wave. The scalar Helmholtz wave equation is defined as

$$\nabla^2 A + k^2\left[1 + \varepsilon_1\left(\vec{r}\right)\right]A = 0 \tag{1}$$

where A is the complex amplitude of the electric field, $\varepsilon_1\left(\vec{r}\right)$ is the deviation from free-space permittivity and characterizes the random variations caused by the plasma irregularities located at $\vec{r}$, and k is the wave number of the incident wave.

Unfortunately, the general solution to equation (1) does not seem to be possible, and one has to settle for various approximate solutions for different applications. An approach, known as parabolic equation method

(PEM), has been developed for the case of normal incidence wave (e.g., Barabenenkov et al., 1971; Yeh & Liu, 1982). The detailed assumptions and mathematical solutions of PEM approach have been well discussed by Yeh and Liu (1982). In the PEM approach one needs to know the plasma irregularity-induced density fluctuations along the propagation path, which in reality is difficult to get. Although an alternative way is to use an ionosphere model for providing the background plasma density and constrained by the in situ measurements from a satellite as irregularity conditions (e.g., Liu et al., 2012), one still cannot precisely model the plasma density fluctuations along the propagation path of a radio wave.

A more practical approach that has been widely used for calculating the scintillation intensity at ground level is the phase screen approximation, which aims to model the primary effect on wave propagation through Fresnel-scale electron density irregularities as a function of the integral of the permittivity fluctuations along the ray path (e.g., Booker et al., 1950; Rino, 1979a, 1979b). In the phase screen model, the plasma irregularity is defined located within an infinitely thin layer. As emerging the irregularity slab, only the phase of incident wave is affected by the random plasma fluctuations. When the wave propagates further downward, the distorted wave front will set up an interference pattern resulting in amplitude fluctuations. The later process is diffraction, and it depends on the random deviations of the curvature of the phase front, which in turn is determined by the size and strength distributions of the plasma irregularities.

The phase screen model basically admits analytic representations of the intensity spectral density function and phase structure function (Carrano & Rino, 2016). As given by Yeh and Liu (1982) and Kintner et al. (2007), the spectrum of the radio wave intensity by amplitude is $I = A * A$:

$$\Phi_I(q) = \Phi_\phi(q)\sin^2\left(\frac{q^2 r_F^2}{8\pi}\right) \tag{2}$$

where Φ_I is the Fourier transform of the intensity autocorrelation function, q is the horizontal wave number of the phase fluctuations across the screen, Φ_ϕ is the power spectrum of the wave phase exciting the screen and for small changes in phase is linearly related to the irregularity density spectrum, and $r_F = \sqrt{2\lambda r}$ is the Fresnel radius, where λ is the incident signal's wavelength and r is the distance from the irregularity slab to the receiver. The term $\sin^2\left(\frac{q^2 r_F^2}{8\pi}\right)$ is the Fresnel filtering function. To the first order, this function provides an upper limit on the scale size of irregularities. The upper limit of the scale size is the Fresnel radius, r_F, occurring when the $\sin^2$ term goes to 1, that the argument is equal to $(2n-1)\,\pi/2$ radians. We see that for a given incident wave with wavelength of λ, after emerging from the irregularity slab, it needs to propagate through a certain distance to have the diffraction process, which further causes amplitude scintillation.

4.2. The GPS Signal Amplitude Fades Observed at Different Altitudes

The GPS signal amplitude fades observed by the spaceborne receivers at different altitudes shown in our study support the assumption of the phase screen model, that the irregularity slab mainly causes the deviation of radio wave phase but not the radio wave amplitude. That is why, as the Swarm and CHAMP fly inside the irregularity slab, almost no signal amplitude fluctuations (less than 2 dB Hz) are observed. When the waves emerge from the slab and continue to propagate to the ground, amplitude fades can reach up to more than 10 dB Hz for receivers at lower altitude (e.g., GOCE) and ground. The signal amplitude degradation exceeding 10 dB Hz observed by the GOCE satellite provides also direct support for the simulation of Xu et al. (2018).

But one difference between the GOCE observations and simulation of Xu et al. (2018) is that the GPS signal amplitude degradation detected by the GOCE onboard receiver shows much smoother variation (see Figure 4a, and we have also found many similar events). One possible reason could be that Xu et al. (2018) used ground-based measurements as model simulation input but not derived directly from a spaceborne receiver. In most cases, the zonal drift velocity of the ionospheric plasma irregularities has a typical value of 100–200 m/s. Considering the irregularities have outer scale sizes of several hundred kilometers, for a ground-based receiver, the received signal within a short time period, for example, within 1 min, should be affected by the same irregularities or at least the irregularities with structures highly correlated. As a result, the time series (within a short period) of a ground-based receiver reflect mainly influences from the same irregularities. However, the LEO satellite moves at a typical speed of about 7.5 km/s, and compared to this velocity the drift of the irregularities itself can be ignored. Within 1 min the LEO satellites can probe

the irregularities at a scale of about 450 km; therefore, the structure of irregularities can change dramatically within such a scale size. As a result, the time series of a spaceborne receiver reflect the influences of irregularities with different structures. Furthermore, the GOCE orbit has an inclination of 96.7°, which means it mainly probes the irregularities along the meridional direction, while the ground-based receiver reflects mainly the zonal structure of the irregularities. This could also contribute to the differences between the observed GOCE signal amplitude degradation and the simulation from Xu et al. (2018).

4.3. Different Scenarios for the Radio Occultation and Topside Receivers

For better modeling the propagation of radio waves through the extended random media, which allows both phase and amplitude fluctuations to accumulate within the medium, the phase screen model has been updated by the multiple phase method (e.g., Knepp, 1983; Grimault, 1998), which is especially important when modeling the radio occultation (RO) experiments through the ionosphere, as the radio wave propagation path inside the random medium can be very long (Carrano et al., 2011). In fact, the GPS signal amplitude scintillation from spaceborne RO antennas has been reported by earlier literatures (e.g., Ko & Yeh, 2010; Uma et al., 2012; Wu et al., 2005). However, the RO antenna is in a different orientation compared to the antenna on the topside of a satellite. The RO antenna only tracks GPS signals with elevation angles lower than the horizon, and therefore the GPS signal has a very long propagating path through the ionosphere (Kursinski et al., 2000; Ware et al., 1996). Ko and Yeh (2010) found two typical signal-to-noise ratio fluctuations of RO measurements. One is of a very short interval (~15 s) when the tangent point height of the occultation ray path is located at *E* region heights (maximum S_4 at ~111 km), and the other one is of a longer time interval (~100 s) when the tangent heights of the occultation ray paths are located at the lower *F* region heights (maximum S_4 at ~270 km). In both situations the irregularities are assumed to be located at the tangent point height, from where the distance to the RO receiver on board LEO satellites is far enough (>100–200 km) to be affected by the Fresnel diffractive process, which further causes the signal amplitude fades. In the model simulation of Xu et al. (2018), for the scenario of an occultation receiver on board a LEO satellite, both phase and amplitude scintillations were observed, which is similar to the ground-based receiver.

5. Summary

In this study we provided a detailed analysis of the received GPS signal amplitude performance from receivers on board LEO satellites at different altitudes. The main findings are summarized as follows:

1. When strong ionospheric plasma irregularities are encountered, the GPS receivers on board Swarm and CHAMP (at about 400–450 km) show both clear carrier phase fluctuations, but almost no amplitude fades (less than 2 dB Hz). The result indicates that it is the strong phase variation that causes the Swarm/CHAMP receivers (located inside the slab of irregularities) to stop tracking the GPS satellites when scintillations happen.
2. For the receiver on board the GOCE satellite at about 250 km, being 100–200 km below the plasma irregularities, events with GPS signal amplitude fades exceeding 12 dB are observed in addition to strong phase variations. By further analyzing 2-year GOCE data, the average signal amplitude degradation reaches 8 dB Hz at both equatorial and polar regions, where transient GPS signal interruptions are frequently observed.
3. These results suggest that the distance from the receiver to the plasma irregularity slab is important, which affects the Fresnel diffractive process in the way to cause the GPS signal amplitude fades.

Acknowledgments
The authors want to thank Shin-Yi Su, Hermann Lühr, and Oliver Montenbruck for fruitful discussions. The European Space Agency (ESA) is acknowledged for providing the Swarm and GOCE data. The servers for distributing the Swarm and GOCE data are https://earth.esa.int/web/guest/swarm/data-access and https://earth.esa.int/web/guest/-/goce-data-access-7219, respectively. The CHAMP mission is sponsored by the Space Agency of the German Aerospace Center (DLR) through funds of the Federal Ministry of Economics and Technology, and the data are accessible at the website (https://isdc.gfz-potsdam.de/champ-isdc/). The work of Chao Xiong is supported by the ESA GOCE-HPF project (Grant 18308/04/NL/MM). Ji-Sheng Xu and Fan Yin are supported by the National Natural Science Foundation of China (Grants 41774163 and 41474157).

References

Aarons, J. (1982). Global morphology of ionospheric scintillations. *Proceedings of the IEEE*, *70*(4), 360–378. https://doi.org/10.1109/PROC.1982.12314

Aarons, J., & Basu, S. (1994). Ionospheric amplitude and phase fluctuations at the GPS frequencies, paper presented at ION GPS, Inst. of Navig., Salt Lake City, Utah.

Barabenenkov, Y. N., Kravtsov, Y. A., Rytov, S. M., & Tatarskii, V. I. (1971). Status of the theory of propagation of waves in a randomly inhomogeneous medium. *Soviet Physics Uspekhi*, *13*(5), 551–575.

Basu, S., Basu, S., Mullen, J. P., & Bushby, A. (1980). Long-term 1.5 GHz amplitude scintillation measurements at the magnetic equator. *Geophysical Research Letters*, *7*(4), 259–262. https://doi.org/10.1029/GL007i004p00259

Bhattacharyya, A., Kakad, B., Sripathi, S., Jeeva, K., & Nair, K. U. (2014). Development of intermediate scale structure near the peak of the *F* region within an equatorial plasma bubble. *Journal of Geophysical Research: Space Physics*, *119*, 3066–3076. https://doi.org/10.1002/2013JA019619

Bock, H., Jaeggi, A., Meyer, U., Visser, P., van den Ijssel, J., van Helleputte, T., et al. (2011). GPS derived orbits for the GOCE satellite. *Journal of Geodesy*, *85*(11), 807–818. https://doi.org/10.1007/s00190-011-0484-9

Booker, H. G., Ratcliffe, J. A., & Shinn, D. H. (1950). Diffraction from an irregular screen with applications to ionospheric problems. *Philosophical Transactions of the Royal Society London, Series A*, *856*, 579–609.

Carrano, C. S., Groves, K. M., Caton, R. G., Rino, C. L., & Straus, P. R. (2011). Multiple phase screen modeling of ionospheric scintillation along radio occultation raypaths. *Radio Science*, *46*, RS0D07. https://doi.org/10.1029/2010RS004591

Carrano, C. S., & Rino, C. L. (2016). A theory of scintillation for two-component power law irregularity spectra: 1. Overview and numerical results. *Radio Science*, *51*, 789–813. https://doi.org/10.1002/2015RS005841

Cheng, J., Xu, J. S., & Cai, L. (2018). A comparison of statistical features of ionospheric scintillations and cycle slips in the mid-south region of China. *Chinese Journal Geophysics (in Chinese)*, *61*(1), 18–29. https://doi.org/10.6038/cjg2018L0065

Grimault, C. (1998). A multiple phase screen technique for electromagnetic wave propagation through random ionospheric irregularities. *Radio Science*, *33*(3), 595–605. https://doi.org/10.1029/97RS03552

Kintner, P. M., Ledvina, B. M., & de Paula, E. R. (2007). GPS and ionospheric scintillations. *Space Weather*, *5*, S09003. https://doi.org/10.1029/2006SW000260

Knepp, D. L. (1983). Multiple phase-screen calculation of the temporal behavior of stochastic waves. *Proceedings of the IEEE*, *71*(6), 722–737. https://doi.org/10.1109/PROC

Ko, C. P., & Yeh, H. C. (2010). COSMIC/FORMOSAT-3 observations of equatorial *F* region irregularities in the SAA longitude sector. *Journal of Geophysical Research*, *115*, A11309. https://doi.org/10.1029/2010JA015618

Kursinski, E. R., Hajj, G. A., Leory, S. S., & Herman, B. (2000). The GPS radio occultation technique. *Terrestrial, Atmospheric and Oceanic Sciences*, *11*(1), 53–114.

Liu, Y. H., Chao, C. K., Su, S.-Y., & Liu, C. H. (2012). Study of a coincident observation between the ROCSAT-1 density irregularity and Ascension Island scintillation. *Radio Science*, *47*, RS5001. https://doi.org/10.1029/2011RS004908

Montenbruck, O., Garcia-Fernandez, M., & Williams, J. (2006). Performance comparison of semi-codeless GPS receivers for LEO satellites. *GPS Solutions*, *10*(4), 249–261. https://doi.org/10.1007/s10291-006-0025-9

Montenbruck, O., & Kroes, R. (2003). In-flight performance analysis of the CHAMP BlackJack GPS Receiver. *GPS Solutions*, *7*(2), 74–86. https://doi.org/10.1007/s10291-003-0055-5

Pi, X., Mannucci, A. J., Lindqwister, U. J., & Ho, C. M. (1997). Monitoring of global ionospheric irregularities using the worldwide GPS network. *Geophysical Research Letters*, *24*(18), 2283–2286. https://doi.org/10.1029/97GL02273

Reigber, C., Luhr, H., & Schwintzer, P. (2002). CHAMP mission status. *Advances in Space Research*, *30*(2), 129–134.

Rino, C. L. (1979a). A power law phase screen model for ionospheric scintillation: 1. Weak scatter. *Radio Science*, *14*(6), 1135–1145.

Rino, C. L. (1979b). A power law phase screen model for ionospheric scintillation: 2. Strong scatter. *Radio Science*, *14*(6), 1147–1155.

Rummel, R., Balmino, G., Johannessen, J., Visser, P., & Woodworth, P. (2002). Dedicated gravity field missions-principles and aims. *Journal of Geodynamics*, *33*(1-2), 3–20. https://doi.org/10.1016/S0264-3707(01)00050-3

Sust M., Zangerl, F., Montenbruck, O., Buchert, S., & Garcia-Rodriguez, A. (2014). Spaceborne GNSS-receiving system performance prediction and validation. In *NAVITEC 2014, ESA Workshop on Satellite Navigation Technologies and GNSS Signals and Signal Processing*. Noordwijk, Netherlands.

Uma, G., Liu, J. Y., Chen, S. P., Sun, Y. Y., Brahmanandam, P. S., & Lin, C. H. (2012). A comparison of the spread-F derived by International Reference Ionosphere and the S4 index observed by FORMOSAT-3/COSMIC during the solar minimum period of 2007–2009. *Earth, Planets and Space*, *64*(6), 467–471.

van den Ijssel, J., Forte, B., & Montenbruck, O. (2016). Impact of Swarm GPS receiver updates on POD performance. *Earth, Planets and Space*, *68*(1), 68–85. https://doi.org/10.1186/s40623-016-0459-4

van den Ijssel, J., Visser, P., Doornbos, E., Meyer, U., Bock, H., & Jäggi, A. (2011). GOCE SSTI L2 losses and their impact on POD performance. In *Proceedings of the 4th international GOCE user workshop* (pp. 1–6). Munich, Germany: ESA SP-696.

Van Dierendonck, A. J., Klobuchar, J., & Hua, Q. (1993). Ionospheric scintillation monitoring using commercial single frequency C/A code receivers. Paper presented at the 6th International Technical Meeting of the Satellite Division of The Institute of Navigation (ION GPS 1993), Salt Lake City, Utah, 22–24 Sept.

Ware, R., Rocken, C., Solheim, F., Exner, M., Schreiner, W., Anthes, R., et al. (1996). GPS sounding of the atmosphere from low Earth orbit-preliminary results. *Bulletin of the American Meteorological Society*, *77*(1), 19–40.

Wu, D. L., Ao, C. O., Hajj, G. A., de la Torre Juarez, M., & Mannucci, A. J. (2005). Sporadic *E* morphology from GPS-CHAMP radio occultation. *Journal of Geophysical Research*, *110*, A01306. https://doi.org/10.1029/2004JA010701

Xiong, C., Stolle, C., & Lühr, H. (2016). The Swarm satellite loss of GPS signal and its relation to ionospheric plasma irregularities. *Space Weather*, *14*, 563–577. https://doi.org/10.1002/2016SW001439

Xiong, C., Stolle, C., Lühr, H., Park, J., Fejer, B. G., & Kervalishvili, G. N. (2016). Scale analysis of the equatorial plasma irregularities derived from Swarm constellation. *Earth, Planets and Space*, *68*(1), 121. https://doi.org/10.1186/s40623-016-0502-5

Xiong, C., Stolle, C., & Park, J. (2018). Climatology of GPS signal loss observed by Swarm satellites. *Annales de Geophysique*, *36*(2), 679–693. https://doi.org/10.5194/angeo-36-679-2018

Xiong, C., Xu, J., Wu, K., & Yuan, W. (2018). Longitudinal thin structure of equatorial plasma depletions coincidently observed by Swarm constellation and all-sky imager. *Journal of Geophysical Research: Space Physics*, *123*, 1593–1602. https://doi.org/10.1002/2017JA025091

Xu, D. Y., Morton, Y., Yu, J., & Rino, C. (2018). Simulation and tracking algorithm evaluation for scintillation signals on LEO satellites traveling inside the ionosphere. In *2018 IEEE/ION position, location and navigation symposium* (pp. 1143–1149). Monterey, CA. https://doi.org/10.1109/PLANS.2018.8373498

Yeh, K. C., & Liu, C. H. (1982). Radio wave scintillations in the ionosphere. *Proceedings of the IEEE*, *70*, 324–360.

Zangerl, F., Griesauer, F., Sust, M., Montenbruck, O., Buchert, B., & Garcia, A. (2014). SWARM GPS precise orbit determination receiver initial in-orbit perfor-mance evaluation. In *Proceedings of the 27th international technical meeting of the satellite division of the institute of navigation (ION GNSS+)* (pp. 1459–1468). Tampa, FL: Tampa Convention Center.